 doi:10.20944/preprints202209.0478.v1

Article

Gain-switched short pulse generation from 1.55 μm InAs/InP/(113)B quantum dot laser modelled using multi-population rate equations

Hilal S. Duranoglu Tunc [1], Nuran Dogru [2,*] and Erkan Cengiz [2]

[1] Dresden University of Technology, Radio Frequency&Photonics Engineering, Dresden, Germany; hilal_sultan.duranoglu_tunc@tu-dresden.de
[2] University of Gaziantep, Electrical & Electronics Engineering, Gaziantep, Turkey; dogru@gantep.edu.tr
* Correspondence: dogru@gantep.edu.tr; Tel.: (+903423172132)

Abstract: For the first time the gain switching properties of an InAs-InP (113)B quantum dot laser are examined theoretically in detail to generate shorter pulses with the application of a Gaussian pulse beam to the laser excited state. The multi population rate equations considering nonlinear gain are solved by the Runge –Kutta method. The numerical results demonstrated that as the homogeneous and the inhomogeneous broadening increase, the differential gain, the gain compression factor and the threshold current of excited state decrease, while threshold current of ground state increases. It was also observed that the contribution of the excited state to gain-switched output pulses depends on not only the value of the inhomogeneous broadening but also the magnitude of the applied current. Finally it was shown that without an optical beam, output pulse has long pulse width due to ground state emission, whereas with an optical beam, narrow pulses having high peak power owing to the excited state emission are generated even though at low currents.

Keywords: gain-switching, semiconductor laser, quantum-dot, homogeneous-broadening, inhomogeneous-broadening, pulse generation

MSC:

1. Introduction

Quantum dot lasers have superior features compared to quantum well counterparts [1–4] such as, temperature independence, low threshold current [5], giving rise to be operated with low chirp for both ground sate (Grs) and excited state (Exs) lasing [4], better resistance values for optical feedback [6]. The feature of being relatively insensitive to temperature makes quantum dot (Q-Dot) lasers to avoid the need for thermoelectric coolers [7]. Since mentioned features makes Q-Dot lasers, compact, cheap, lightweight and low power systems, they are appropriate candidates for applications in optical communications [7].

Studies [3, 8–9] revealed that in order to realize optical communication with low loss, it is appropriate to use InAs-InP Q-Dot lasers that can radiate at 1.55 μm wavelength instead of InGaAs-GaAs QD lasers, which cannot radiate above 1.45μm wavelength. Although mode-locking and Q-switching are the some methods to obtain short pulses, the gain switching method is ahead of its alternatives in practice since it allows for lower cost and simpler manufacturing. Considering all the convenience it offers in practice, in this study, the issue of producing short pulses with the gain switching method has been investigated theoretically.

When studies on obtaining short pulses using gain switching method from InAs-InP QD lasers are examined, it was found that there is no detailed study which takes into consideration of nonlinear gain and which based on multi-population rate equations.

Preprints (www.preprints.org) | NOT PEER-REVIEWED | Posted: 30 September 2022 doi:10.20944/preprints202209.0478.v1

Since obtaining short pulse is of great importance in optical communication, we have proposed a method which includes a simultaneous application of an external optical Gaussian beam (EOGB) to Exs and an injection current to the wetting layer (Wly) of the Q-Dot laser to obtain shorter pulses at low injection currents. Although, Q-Dot lasers have superior performance, they cannot always satisfy the expected features in reality due to the homogeneous broadening, the inhomogeneous broadening and the gain compression factor [10–12]. To obtain an appropriate and suitable approach to experimental results by theoretically, as many aspects of real experiment as possible should be taken into account when performing the simulation. For this, the effect of the homogeneous and the inhomogeneous broadening with the effect of the gain compression were taken into consideration in this study. Therefore, this paper is organized as follows: Section 2 introduces the theoretical description of multi population rate equations for direct relaxation model considering the nonlinear gain case. The obtained results discussed in section 3 shows that by applying an EOGB into the Exs, narrow pulses having a pulse width of around 26 ps with high peak power, are generated due to the Exs emissions even though at low currents. In addition, it was shown that the contribution of excited state to gain switched output pulses does not depend on only the value of the inhomogeneous broadening but also on the magnitude of the applied current. Furthermore, the effect of homogeneous and inhomogeneous broadenings on the differential gain, the gain compression factor and the threshold current is also investigated. Finally, our results are summarized and conclusions in section 4.

2. Materials and Methods

The laser model used in this study for InAs-InP(113)B Q-Dot is based on the multi population rate equations for direct relaxation model described in [2, 11, 13]. The rate equations were solved using the Runge–Kutta method to investigate the carrier dynamics in the two lowest energy levels, Grs and Exs. While performing our study, we have neglected the effect of temperature and carrier loss. We assumed that the carriers were directly injected from the contacts to the Wly; therefore, the carrier dynamics were not considered in the barrier. Direct transition from the Wly to the Grs was introduced to reproduce the experimental results [2, 11, 13]. Q-Dot active region consists of Q-Dots ensemble having different sizes. In the model, in order to consider effect of the inhomogeneous broadening (Γ_{ihom}), Q-Dot ensemble is divided into 2X+1 groups, depending on their resonant energies for the interband transition [14–15]. Fig. 1 shows the relaxation mechanisms in the xth Q-Dot subgroup. Energies of Exs and Grs of xth Q-Dot are represented as E_{Exs_x} and E_{Grs_x}, respectively. As a result, longitudinal cavity photon modes of up to 2P+1 are constructed in the cavity [13]. When the index x is equal to X, this situation corresponds to the central Q-Dot group. When index p is equal to P, this case corresponds to the central mode with the transitional energies of E_{Exs0} and E_{Grs0} for Exs and Grs, respectively. Each Q-Dot group energy width (ΔE) and mode energy separation (ΔE_p) are assumed to be equal and taken to be as a 1meV [13]. xth Q-Dot group energy and pth mode energies are indicated by

$$E_{Exs\_x\,,Grs\_x} = E_{Exs0\,,Grs0} - (X - x)\Delta E \quad x = 1,2,\dots,2X+1 \tag{1}$$

$$E_{Exs\_p\,,Grs\_p} = E_{Exs0\,,Grs0} - (P - p)E_p \quad p = 1,2,\dots,2P+1 \tag{2}$$

Preprints (www.preprints.org) | NOT PEER-REVIEWED | Posted: 30 September 2022 doi:10.20944/preprints202209.0478.v1

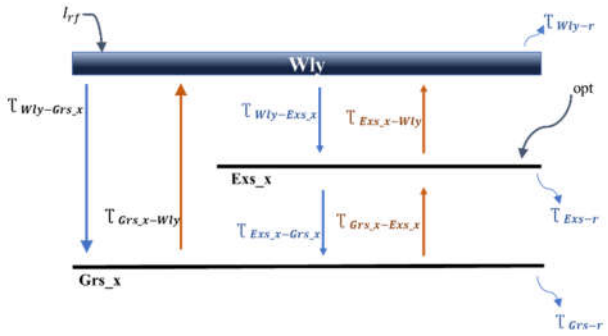

Figure 1. Schematic representation of carrier dynamics for xth QD subgroup.

When injection current I is applied to Wly of Q-Dot laser, by the effect of injection current, some carriers move to the lower state E_{Exs-x} and E_{Grs-x} with a capture time of $\tau_{Wly-Exs\_x}$ for the transition from Wly to E_{Exs_x} and a relaxation time of $\tau_{Wly-Grs\_x}$ for the Wly to the E_{Grs_x} transition. Some photons are emitted from the Wly due to spontaneous emission over a time τ_{Wly-r}. However, in the Exs, some carriers are relaxed into the E_{Grs_x} with a relaxation time $\tau_{Exs\_x-Grs\_x}$. Further, the more energetic carriers are thermally transferred to the Wly with a time τ_{Exs_x-Wly}. The other carriers recombine spontaneously with an emission time τ_{Exs-r} or by stimulated emission of photons. The same mechanism for the carrier dynamics transitions is applied at the Grs level. The same processes occur for the carrier population in the Grs level with regard to the Exs.

The capture and relaxation times can be calculated [13] as

$$\tau_{Wly-Exs\_x} = \frac{1}{(A_{Wly}+(C_{Wly}N_{Wly}))(1-f_{Exs\_x})(G_{xExs})} \quad (3)$$

$$\tau_{Exs\_x-Grs\_x} = \frac{1}{(A_{Exs}+(C_{Exs}N_{Wly}))(1-f_{Grs\_x})} \quad (4)$$

$$\tau_{Wly-Grs\_x} = \frac{1}{(A_{Wly}+(C_{Wly}N_{Wly}))(1-f_{Grs\_x})(G_{xGrs})} \quad (5)$$

Here N_{Wly} is the carrier density in the Wly, $A_{Wly,Exs}$, $C_{Wly,Exs}$ are the phonon and Auger coefficients in Wly and Exs, respectively. Their values are estimated experimentally [16]. f_{Exs_x,Grs_x} is the occupation probabilities in xth group of Q-Dot in the Exs and Grs.

$$f_{Exs\_x} = \frac{N_{Exs\_x}}{\mu_{Exs}N_O G_{xExs}}, f_{Grs\_x} = \frac{N_{Grs\_x}}{\mu_{Grs}N_O G_{xGrs}} \quad (6)$$

$\mu_{Exs,Grs}$ is the degeneracy of the Exs and Grs, N_o is the Q-Dot density and $N_{Exs\_x,\ Grs\_x}$ is the carrier density in the Exs and Grs of xth Q-Dot. $G_{xExs,xGrs}$ is the density rate of xth Q-Dot in the Exs and Grs. To calculate $G_{xExs,xGrs}$, the Q-Dot size distribution is assumed to be a Gaussian function given as

$$G_{xExs,xGrs} = G_{inh,Exs,Grs}(E_{Exs\_x,Grs\_x} - E_{Exs0,Grs0})\Delta E \quad (7)$$

$$G_{inh,Exs,Grs}(E_{Exs\_x,Grs\_x} - E_{Exs0,Grs0}) = \frac{1}{\sqrt{2\pi}\sigma} exp\left(-\frac{(E_{Exs\_x,Grs\_x}-E_{Exs0,Grs0})^2}{2\sigma^2}\right) \quad (8)$$

Full width half maximum of Gaussian function is given as Γ_{inh}=2.35σ. In other word Γ_{inh} is described as inhomogeneous broadening.

Carrier escape time is related to carrier capture time [17] and given as

$$\tau_{Exs\_x-Wly} = \tau_{Wly-Exs\_x}\frac{\mu_{Exs}}{\mu_{Wly}} e^{(E_{Wly}-E_{Exs\_x})/k_BT} \quad (9)$$

Preprints (www.preprints.org) | NOT PEER-REVIEWED | Posted: 30 September 2022 doi:10.20944/preprints202209.0478.v1

$$\tau_{Grs\_x-Wly} = \tau_{Wly-Grs\_x}\frac{\mu_{Grs}}{\mu_{Wly}}e^{(E_{Wly}-E_{Grs\_x})/k_BT} \tag{10}$$

$$\tau_{Grs\_x-Exs\_x} = \tau_{Exs\_x-Grs\_x}\frac{\mu_{Grs}}{\mu_{Exs}}e^{(E_{Exs\_x}-E_{Grs\_x})/k_BT} \tag{11}$$

Change in the carrier density in the Wly, Exs and Grs and change in the photon density in the Exs and Grs for multi modes rate equations are given as

$$\frac{dN_{Wly}}{dt} = \frac{I}{qV} + \sum_x \frac{N_{Exs\_x}}{\tau_{Exs\_x-Wly}} + \sum_x \frac{N_{Grs\_x}}{\tau_{Grs\_x-Wly}} - \frac{N_{Wly}}{\overline{\tau_{Wly-Exs}}} - \frac{N_{Wly}}{\overline{\tau_{Wly-Grs}}} - \frac{N_{Wly}}{\tau_{Wly-r}} \tag{12}$$

$$\frac{dN_{Exs\_x}}{dt} = \frac{N_{Wly}}{\overline{\tau_{Wly-Exs\_x}}} + \frac{N_{Grs\_x}(1-f_{Exs\_x})}{\tau_{Grs\_x-Exs\_x}} - \frac{N_{Exs_x}}{\tau_{Exs_x-Grs_x}} - \frac{N_{Exs_x}}{\tau_{Exs_x-Wly}} - \frac{N_{Exs_x}}{\tau_{Exs-r}} - \Gamma v_g \frac{\sum_p g_{pxExs} S_{Exsp}}{1+\varepsilon_{Exsp} S_{Exsp}} +$$

$$\Gamma v_g \frac{(1-f_{Exs\_x})g_{pxExs}}{(2f_{Exs\_x}-1)} opt \tag{13}$$

$$\frac{dN_{Grs\_x}}{dt} = \frac{N_{Wly}}{\overline{\tau_{Wly-Grs}}} + \frac{N_{Exs\_x}}{\tau_{Exs\_x-Grs\_x}} - \frac{N_{Grs\_x}(1-f_{Exs\_x})}{\tau_{Grs\_x-Exs\_x}} - \frac{N_{Grs\_x}}{\tau_{Grs\_x-Wly}} - \frac{N_{Grs\_x}}{\tau_{Grs-r}} - \Gamma v_g \frac{\sum_p g_{pxGrs} S_{Grsp}}{1+\varepsilon_{Grsp} S_{Grsp}} \tag{14}$$

V is the volume, q is the charge, Γ is the confinement factor and v_g is the group velocity. $\overline{\tau_{Wly-Exs}}$, and $\overline{\tau_{Wly-Grs}}$ indicate the average capture times from Wly to Exs and from Wly to Grs in Q-Dot ensemble.

$$\overline{\tau_{Wly-Exs}} = \sum_x \frac{1}{(A_{Wly}+(C_{Wly}N_{Wly})(1-f_{Exs\_x})(G_{xExs})} \tag{15}$$

$$\overline{\tau_{Wly-Grs}} = \sum_x \frac{1}{(A_{Wly}+(C_{Wly}N_{Wly})(1-f_{Grs\_x})(G_{xGrs})} \tag{16}$$

Nonlinear-gain in Exs and Grs is given as

$$g_{pxExs} = \mu_{Exs}\frac{\pi q^2\hbar}{cn_r\varepsilon_0 m_0^2} N_o \frac{|P^{\sigma}_{Exs}|^2}{E_{Exs\_x}}(2f_{Exs\_x}-1)G_{xExs}L_{Exs}(E_{Exs\_p}-E_{Exs\_x})\frac{1}{1+\varepsilon_{Exsp}S_{Exsp}} \tag{17}$$

$$g_{pxGrs} = \mu_{Grs}\frac{\pi q^2\hbar}{cn_r\varepsilon_0 m_0^2} N_o \frac{|P^{\sigma}_{Grs}|^2}{E_{Grs_x}}(2f_{Grs\_x}-1)G_{xGrs}L_{Grs}(E_{Grs\_p}-E_{Grs\_x})\frac{1}{1+\varepsilon_{Grsp}S_{Grsp}} \tag{18}$$

c, ε_o, $\hbar$, and m_o are the speed of light, dielectric constant in free space, Planck constant and free mass of electron, respectively. $|P^{\sigma}_{Exs,Grs}|^2$, is the transfer matrix momentum [10] and it is estimated approximately $2m_oE_{Exs0,Grs0}$ for InAs [17]. S_{Exs_p,Grs_p} is the photon density of pth mode emitted from Exs and Grs. Homogeneous broadening of the stimulated emission process assumed to be Lorentzian such that $L_{Exs,Grs}(E_{Grs\_p}-E_{Grs\_x})$,

$$L_{Exs,Grs}(E_{Exs\_p,Grs\_p}-E_{Exs\_x,Grs\_x}) = \frac{\Gamma_{hom}/\pi}{(E_{Exs\_p,Grs\_p}-E_{Exs\_x,Grs\_x})^2+(\Gamma_{hom})^2} \tag{19}$$

Γ_{hom} is the full-width half maximum of homogeneous broadening.

Gain saturation parameter, $\varepsilon_{Exsp,Grsp}$ of the Exs and Grs is given as

$$\varepsilon_{Exsp,Grsp} = \frac{hq^2\tau_p|P^{\partial}_{Exs,Grs}|^2\Gamma}{2n_r^2\epsilon_0 m_0^2 E_{Exs\_p,Grs\_p}} L_{Exs,Grs}(E_{Exs\_p,Grs\_p}-E_{Exs0,Grs0}) \tag{20}$$

Here τ_p, and n_r indicate the photon life time and refractive index of laser, respectively. $L_{Exs,Grs}(E_{Exs\_p,Grs\_p}-E_{Exs0,Grs0})$ is the Lorentzian function and given as

$$L_{Exs,Grs}(E_{Exs\_p,Grs\_p}-E_{Exs0,Grs0}) = \frac{\Gamma_{hom}/\pi}{(E_{Exs\_p,Grs\_p}-E_{Exs0,Grs0})^2+(\Gamma_{hom})^2} \tag{21}$$

Preprints (www.preprints.org) | NOT PEER-REVIEWED | Posted: 30 September 2022 doi:10.20944/preprints202209.0478.v1

Photon density in Exs and Grs is expressed as

$$\frac{dS_{Exsp}}{dt} = \Gamma v_g \frac{\sum_x g_{pxExs} S_{Exsp}}{1+\varepsilon_{Exsp} S_{Exsp}} - \frac{S_{Exsp}}{\tau_p} + \beta \sum_x \left(L_{Exs} \left(E_{Exs\_p} - E_{Exs\_x} \right) \frac{N_{Exs}}{\tau_{Exs-r}} \right) \Delta E_p \quad (22)$$

$$\frac{dS_{Grsp}}{dt} = \Gamma v_g \frac{\sum_p g_{pxGrs} S_{Grsp}}{1+\varepsilon_{Grsp} S_{Grsp}} - \frac{S_{Grsp}}{\tau_p} + \beta \sum_x \left(L_{Grs} \left(E_{Grs\_p} - E_{Grs\_x} \right) \frac{N_{Grs}}{\tau_{Grs-r}} \right) \Delta E_p \quad (23)$$

Where β is the spontaneous coupling factor.

opt in equation 13 is the photon density for applied EOGB to Exs in a round-trip time. It is defined as

$$opt = \frac{P_i (2L/v_g)}{E_{Exs\_x} * V} \quad (24)$$

P_i is the peak power of applied optical beam and L is the laser cavity length.

3. Discussion

A 1.55 μm InAs-InP (113)B Q-Dot laser was used in the simulation. The following equation was used to calculate the applied AC current *I*, with frequency f and amplitude I_{rf}:

$I(t) = \frac{I_{rf}}{2} (|\cos(2\Pi f t)| - \cos(2\Pi f t))$ [18–19].

The parameters used in the simulations are given in Table 1. The values of these parameters were obtained from [13, 20–22]. Unlike previous studies, here the nonlinear gain was considered for multi-population rate equations.

X and P are taken as X=P=1 (i.e it was assumed that there are 3 Q-Dot ensembles) and an Γ_{hom} of 15 meV and Γ_{ihom} of 45 meV has been used in the following results unless stated otherwise. For these values the gain compression factor, $\varepsilon_{Exsp,Grsp}$ is calculated as 7.8×10^{-16} cm^3 for Exs and Grs.

Since Γ_{hom} and Γ_{ihom} affect the threshold current (I_{th}), the differential gain and the gain compression factor [10, 12], first without EOGB the effect of Γ_{hom} and Γ_{ihom} on these mentioned parameters were investigated. Subsequently, an EOGB was applied to the Exs to observe how the optical beam illumination affects the gain-switching output pulses.

I_{th} was calculated as 30 mA for Exs and 2 mA for Grs for linear gain case ($\varepsilon_{Exs,Grs}=0$) (see in Fig. 2a). 21 mA for Exs and 2 mA for Grs for nonlinear gain case ($\varepsilon_{Exs,Grs}\neq 0$) were obtained (see in Fig. 2b). The total threshold current (Grs+Exs) for both cases was calculated as 2 mA. As seen in the Fig. 2b deviation from the Fig. 2a due to $\varepsilon_{Exs,Grs}$ is because of direct relaxation from Wly to Grs.

Γ_{ihom} changes between 30–80 meV at room temperature [23–24], therefore, we changed it from 30 meV to 80 meV. In this case Γ_{hom} is taken as to be 15 meV at room temperature [11]. Similarly, since range of Γ_{hom} is between 10–30 meV [2], Γ_{hom} is changed from 10 to 30 meV and Γ_{ihom} is taken to be as 45 meV.

For the center subgroup of the Q-Dot (2nd subgroup) when Γ_{ihom} is changed from 30 meV to 80 meV, as I_{th} of Exs drops from 27 mA to 10 mA, I_{th} of Grs increases from 1 mA to 6 mA (see in Fig. 3). If Γ_{ihom} is greater than 70 meV, the threshold current increases as the photon density of Grs decreases, finally threshold currents of Grs and Exs become the same at 11 mA. As seen in Fig. 4 as Γ_{ihom} increases, the differential gain of Exs and Grs decreases. Similar results were also observed in [12].

Preprints (www.preprints.org) | NOT PEER-REVIEWED | Posted: 30 September 2022 doi:10.20944/preprints202209.0478.v1

Table 1. Q-Dot laser parameters

Cavity length, L	0.245 cm
Cavity width, w	12 μm
Confinement factor, Γ	0.025
Quantum dot density, No	$6x10^{16}$ cm^{-3}
Refractive index, nr	3.27
Cavity internal loss, αint	6 cm^{-1}
Mirror reflectivity, R1, R2	0.95, 0.05
Spontaneous emission ofWly, τwr	500ps
Spontaneous emission of Exs , τer	500ps
Spontaneous emission of Grs, τp	1.2ns
Photon lifetime, τr	8.92 ps
Spontaneous coupling factor, β	$1x10^{-4}$
Emission energy of Wly, Ewly	1.05 eV
Emission energy of Exs, Eexs	0.840 eV
Emission energy of GS, Egrs	0.792 eV
Phonon relaxation of Wly, Awly	$1.35x10^{10}$ s^{-1}
Auger coefficient of Wly, Cwly	$5x10^{-9}$ cm^3s^{-1}
Phonon relaxation of Wly, Aexs	$1.5x10^{10}$ s^{-1}
Auger coefficient of Exs, Cexs	$9x10^{-8}$ cm^3s^{-1}
Degeneracy of Grs, Exs, Wly, μgrs,exs,wly	2,4,10
Operating frequency, f	1 GHz
Wavelength, λ	1.55 μm
Homogeneous broadening, Γhom	15 meV
Inhomogeneous broadening, Γihom	45 meV

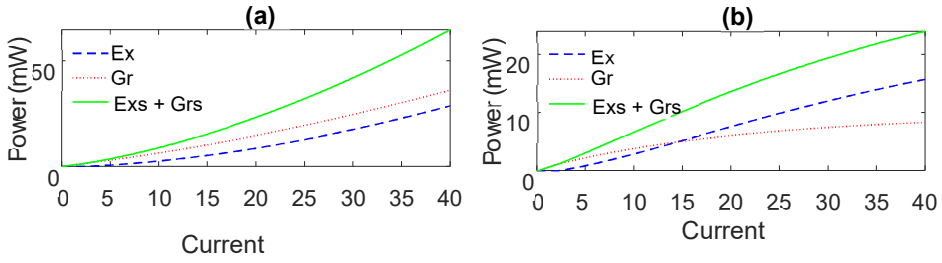

Figure 2. Output power versus dc current without applying EOGB to the Exs, (a) $\varepsilon_{Exs,Grs}=0$ (b) $\varepsilon_{Exs,Grs}\neq 0$.

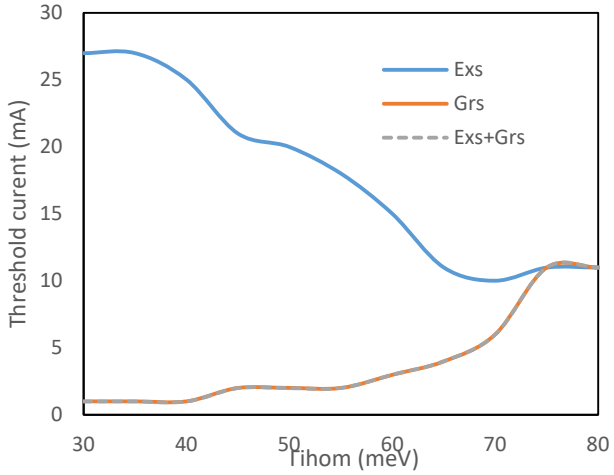

Figure 3. Variation of the threshold current as a function of Γ_{ihom}.

Preprints (www.preprints.org) | NOT PEER-REVIEWED | Posted: 30 September 2022 doi:10.20944/preprints202209.0478.v1

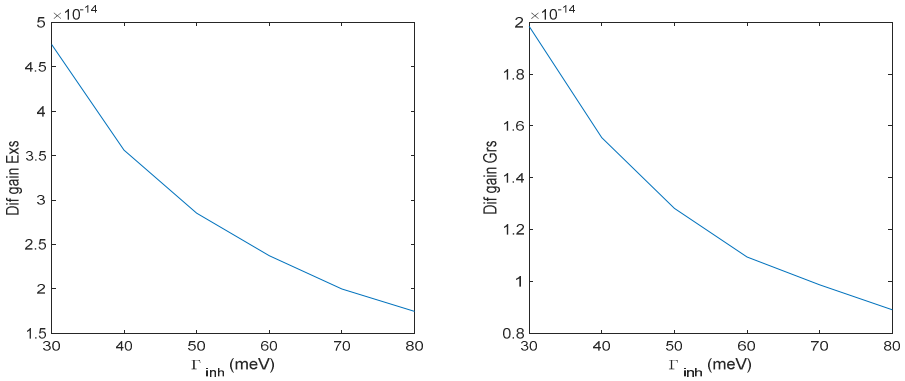

Figure 4. Variation of differential gain as function of the Γ_{ihom} for I_{rf}=40 mA.

Behavior of Γ_{hom} on I_{th} and on differential gain is similar to that of Γ_{ihom}, giving the similar differential gain characteristics as in Fig. 4 when Γ_{hom} is increased from 10 meV to 30 meV. For the center subgroup of the Q-Dot as Γ_{hom} is increased from 10 meV to 30 meV, I_{th} of Exs decreases up to 22.5 meV (dropping from 26 mA to 10 mA) and after that point it slightly increases. I_{th} of Grs increases from 1 mA to 6 mA (see in Fig. 5). When Γ_{hom} is greater than 22.5 meV, the photon density of Grs decreases whereas the threshold current increases, yielding a threshold current of 14 mA, which is equal to that of the Exs. As shown in Fig. 6 the gain compression factor decreases with increasing the Γ_{hom}.

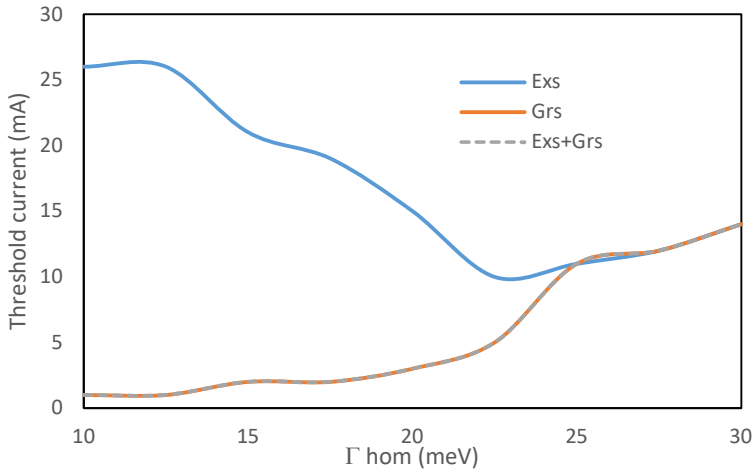

Figure 5. Variation of the threshold current as a function of Γ_{hom}.

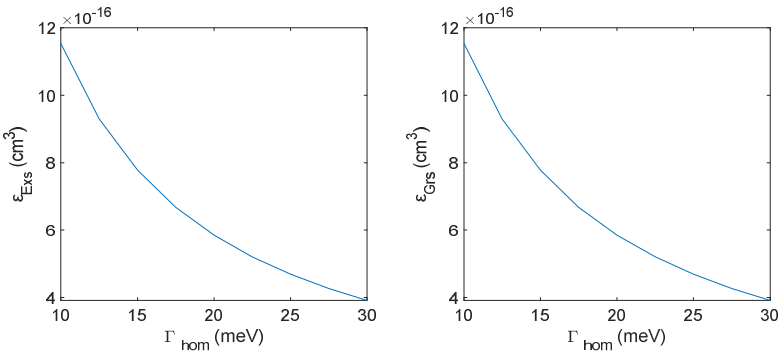

Figure 6. Variation of gain compression factor as function of the Γ_{hom} for I_{rf}=40 mA.

As seen the results, the differential gain of Exs is greater than that of the Grs. Because

Preprints (www.preprints.org) | NOT PEER-REVIEWED | Posted: 30 September 2022 doi:10.20944/preprints202209.0478.v1

degeneracy of the Exs is twice that of the Grs. However, the gain compression factor is the same for Grs and Exs. Our results also showed that the output power decreases with the increasing Γ_{hom} and Γ_{ihom}.

As mentioned before threshold current was obtained 2 mA for the Grs and 24 mA for the Exs for the nonlinear gain case. Therefore, to observe the gain switched output pulses and also simultaneous emission from the Grs and the Exs we applied I_{rf} of 40 mA. Fig. 7 indicates the gain switched output pulses for an I_{rf} of 40 mA. As shown in the figures the Grs pulse width is longer (370 ps), while the Exs pulse width is narrow (43 ps). As seen in the figure the Exs and Grs together contribute to the output pulses since the applied current magnitude is greater than the threshold currents of both states. Therefore, the generated pulses are due to both Exs and Grs emission. The total (Exs+Grs) pulse width is 255 ps and the peak power is 28 mW.

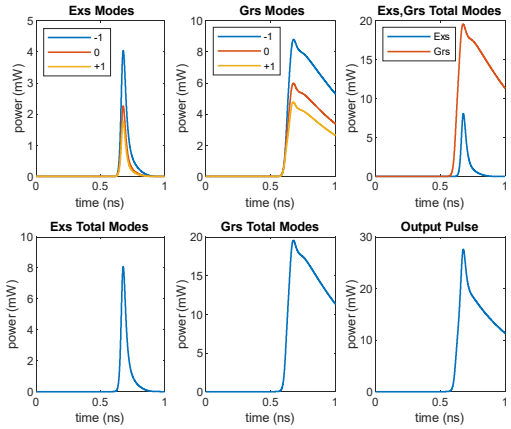

Figure 7. Output pulses for an I_{rf} current of 40 mA.

It was observed that, increasing in injection current leads both peak power and pulse width to increase. Since, the power of the pulse obtained as a result of Grs emission gradually decreased after reaching the highest value, while the power of the pulse obtained as a result of Exs emission decreased rapidly after reaching the maximum value, when the applied injection current is increased, pulse width of the gain-switched pulse increases due to the emission originated from Grs. However, the output pulse due to Exs emission produces shorter pulses due to the Exs photon density decreases rapidly after reaching its maximum value. When the emission of Exs and Grs together form the output pulse, output pulse width expands due to the long pulse width of the Grs photons. Based on these observations, photons emitted from InP Grs can be shown as the reason why the pulses obtained from InAs-InP lasers have long widths in the case of double emission.

It was found that, Grs emission goes saturation while Exs emission continues increasing for InGaAs-GaAs lasers [22]. As a result of this feature, if the injection current is increased, Exs emission becomes dominant in output pulse, yielding shorter pulses. Investigation on InAs-GaAs monolithic Q-Dot lasers revealed that, when the applied injection current increases, width of gain switched pulse decreases [25]. However, since Grs emission does not go to saturation completely for InAs-InP (113)B lasers (see Fig. 2) with the

Preprints (www.preprints.org) | NOT PEER-REVIEWED | Posted: 30 September 2022 doi:10.20944/preprints202209.0478.v1

increasing injection current, both Grs and Exs emissions form the output pulse. As mentioned earlier, the increase in applied injection current causes width of the pulse to expand for InAs-InP lasers as the photons emitted from Grs produce wider output pulses, contrary to InAs-GaAs counterparts.

Wang et. al [12] showed that effect of the inhomogeneous broadening exhibits two distinct regimes. If Γ_{ihom} smaller than the energy difference between Exs and Grs (ΔE_{dif} =E_{Exs0}-E_{Grs0}) lasing occurs only due to Grs, if Γ_{ihom} greater than the ΔE_{dif}, both Grs and Exs contribute the lasing process. However, our results showed that as Γ_{hom} and Γ_{ihom} increase, I_{th} of Exs decreases whereas I_{th} of Grs increases (see in Fig. 3 and 5). Therefore, according to magnitude of the applied current, even if smaller value of Γ_{ihom}, contribution of Exs to output pulses is possible. In order to show this case 25 mA of I_{rf} current is applied and the gain-switched output pulses were obtained for Γ_{ihom}= 30 meV ($\Gamma_{ihom} < \Delta E_{dif}$ =48 meV) and Γ_{ihom}= 55 meV ($\Gamma_{ihom} > \Delta E_{dif}$ =48 meV). As seen in Fig. 8 and 9 output pulse with a full width half maximum (FWHM) of 386 ps and peak power of 26 mW for Γ_{ihom}= 30 meV is generated from Grs emission only. However, since I_{th} of Exs decreased for Γ_{ihom}= 55 meV, both Grs and Exs contribute the output pulse giving an FWHM of 233 ps and peak power of 10 mW. If we apply a current greater than the peak current of 25 mA, for example 60 mA for Γ_{ihom}= 30 meV, both Grs and Exs contribute lasing process simultaneously as shown in Fig. 10 producing a FWHM of 478 ps and peak power of 53 mW. Briefly, we can say that contribution of Exs to gain switched output pulses depend on not only the value of Γ_{ihom}, which is smaller or greater than the energy difference between Exs and Grs, but also on the magnitude of the applied current. In addition, it can be also observed from the results that width of pulses are long due to dominant effect of the Grs emission.

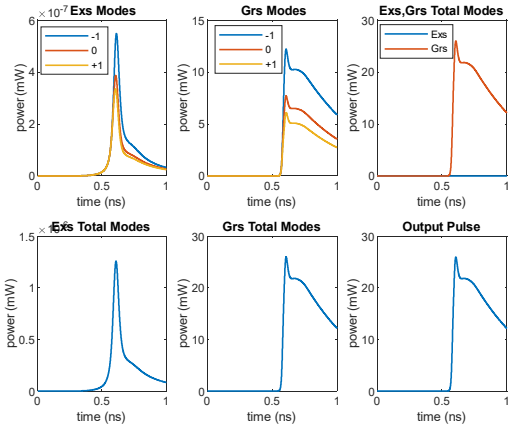

Figure 8. Output pulses for an I_{rf} current of 25 mA for Γ_{ihom}=30 meV.

Preprints (www.preprints.org) | NOT PEER-REVIEWED | Posted: 30 September 2022 doi:10.20944/preprints202209.0478.v1

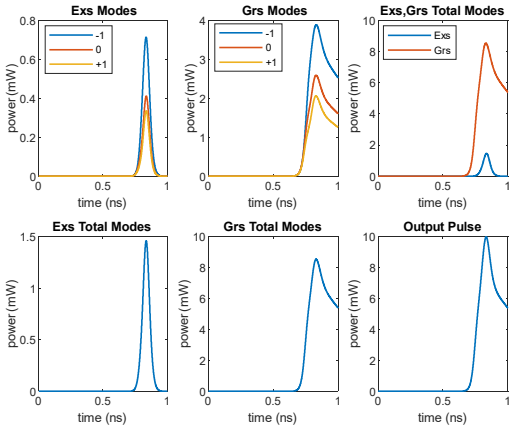

Figure 9. Output pulses for an I_{rf} current of 25 mA for Γ_{ihom}=55 meV.

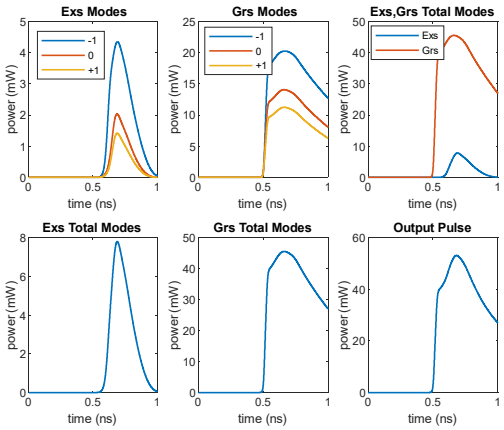

Figure 10. Output pulses for an I_{rf} current of 60 mA for Γ_{ihom}=30 meV.

Based on the results we have obtained, we can say that it is impossible to generate short pulses with high peak power as long as Grs emission is dominant in the output pulse, for InAs-InP QD lasers. Since, threshold current of Exs is much higher than that of Grs, increasing injection current to make Exs emission dominant in gain switched pulse fails. Therefore, in order to obtain gain switched short pulses with high peak power, Exs emission must be sustained while Grs emission must be suppressed, concurrently. To provide these two conditions, application an EOGB to Exs of the laser was performed. Application of EOGB to Exs of the laser results in decreasing threshold currents of both Exs and Grs to zero, related to the peak value of the applied EOGB. Additionally, photon density of Exs can exceed that of Grs up to a certain current range. This condition gives opportunity to obtain gain switched pulses with narrow and high peak power values.

Fig. 11 shows light versus dc current characteristics obtained by applying an EOGB with a peak power of 10 mW and a width of 10 ps. In order to see zero threshold current for both the states dc current was applied up to 50 mA. As seen in the figure the power of Exs is greater than that of the Grs up to some current value with the application of optical beam and the threshold currents become zero for both states.

Preprints (www.preprints.org) | NOT PEER-REVIEWED | Posted: 30 September 2022 doi:10.20944/preprints202209.0478.v1

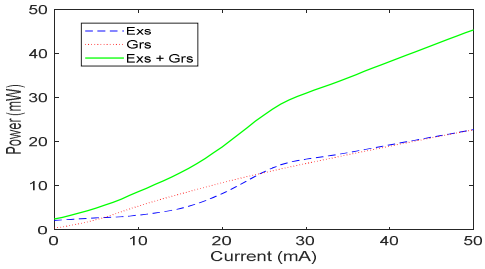

Figure 11. Output power versus dc current under the EOGB illumination. The peak power is 10 mW.

Fig. 12 indicates the gain-switched output pulses under the optical beam having a peak power of 10 mW and a width of 10 ps for I_{rf} of 12 mA. As seen in the figure Exs emission is dominant over Grs emission that means output pulse is generated due to Exs emission. Therefore, width of output pulse is narrow (26 ps) and peak power is high (82 mW) even though the applied current is low. Also, the peak power of EOGB must be increased to further increase the peak power of the output pulse. Fig. 13 shows output pulses for an optical beam peak power of 20 mW for I_{rf} of 12 mA. As seen the figure while peak power of the output increases, width of the output pulse slightly increase giving a value of 27 ps.

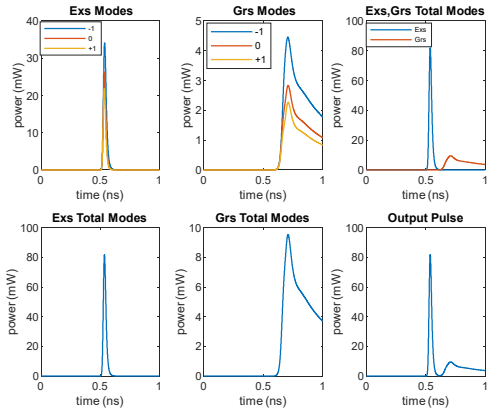

Figure 12. Output pulse under the illumination of an EOGB of 10 mW for I_{rf}=12 mA.

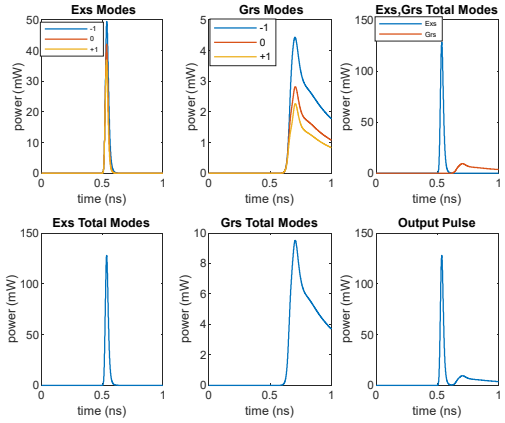

Figure 13. Output pulse under the illumination of an EOGB of 20 mW for I_{rf}=12 mA.

 doi:10.20944/preprints202209.0478.v1

Our results also showed that changes in the laser parameters does not affect the output pulse width and peak power significantly in presence of the optical beam. However, without EOGB the output pulses are strongly affected by the change in the laser parameters. Similar results were also obtained for InAs-InP (113)B quantum dot laser based on single mode rate equations [26].

Regarding the zero gain compression factor our results demonstrated that behavior of gain switching characteristics with and without EOGB are similar for liner gain and nonlinear gain cases except that higher peak power and narrower output pulses are obtained for linear gain case.

As a conclusion, when an EOGB is applied to the Exs, the photon emission of Exs becomes dominant over the Grs, giving shorter output pulses having a high peak power. The Exs emission can be tuned to make it suitable for optical communication [27–28].

4. Conclusion

In this study, for the first time, the gain switching properties have been investigated in detail theoretically in the absence and presence of optical beam illumination for direct relaxation model of InAs-InP (113)B Q-dot lasers based on multi population rate equations. First effect of the homogeneous and the inhomogeneous broadenings on the differential gain, the gain compression factor and the threshold current was examined in the absence of optical beam. Subsequently, gain-switched output pulses were studied in the absence and presence of optical beam illumination. Our results indicated the followings:

1) The differential gain and the gain compression factor decrease with the increasing the homogeneous and the inhomogeneous broadenings. However, while the threshold current of the ground state increases, that of the excited state decreases as the broadenings are increased.

2) While emission of ground state produces the gain switched pulses at small currents (smaller than the threshold current of excited state), emissions of Exs and Grs contribute to the output pulses at greater currents values (greater than the threshold currents of both excited state and ground state). Since, photon density of ground state decrease gradually after reaching its maximum value, output pulses originated from ground state emission have long pulse widths. On the other hand, photon density of excited state decreases rapidly after reaching its maximum value. Therefore, excited state emission gives opportunity to obtain shorter pulses by using InAs-InP quantum dot lasers. Application of a Gaussian shaped external optical beam to the excited state of the laser results in shorter pulses with high peak power, since it suppresses ground state emission and sustains excited emission, simultaneously.

3) The contribution of excited state to gain switched output pulses depends on the value of inhomogeneous broadening as well as on the magnitude of the applied current.

As a result, short pulses with a width of around 26 ps with a high peak power can be generated at low currents by applying an external optical beam to the Exs. These results showed that InAs-InP (113)B quantum dot lasers is a candidate source for many applications as well as optical communication systems.

 doi:10.20944/preprints202209.0478.v1

References

1. Shimizu M, Suzuki Y, and Watanabe M, *Jpn. J. Appl. Phys.* **1998**, 37 L, 1040–L.
2. Grillot F, Veselinov K, Gioannini M, Montrosset I, Even J, Piron R, Homeyer E, and Louaiche S *IEEE J. of Quantum Electron*. **2009**, 45, 872.
3. Caroff P, Paranthoen C, Platz C, Dehaese O, Folliot H, Bertru N, Labbe C, Piron R, Homeyer E, Le Corre A, and Louaiche S *J. Appl. Phys*. **2005**, 87**,** 243107.
4. Saito H, Nishi K, Kamei A, and Sugou S, *IEEE Photon. Technol. Lett.* **2000**, 12, 1298.
5. Reithmaier J. P and Forchel A *Comptes Rendus Physique*, **2003**, 4, 611.
6. Huang H, Duan J, Jung D, Liu A Y, Zhang Z, Norman J, Bowers J E, and Frédéric Grillot *J. Opt. Soc. Am. B,* **2018**, 35, 2780.
7. Rafailov E U, Cataluna M A , and Sibbett W *Nature photonics* **2007**, 1.7, 395-401.
8. Sritirawisarn N, Otten F W M, van, Eijkemans T J , and Nötzelet R *J. Crystal Growth.* **2007**, 305, 63.
9. Heck S C, Osborne S, Healy S B , O'Reilly E P, Lealarge F, Pointgt F, Le Gouezigou O, and Accard A *IEEE J. Quantum. Electronics.* **2009**, 45, 1508.
10. Sugawara M, Mukai K, Nakata Y and Ishikawa H *Phys. Rev.* **2000***, B*. 61, 7595.
11. Grillot F, Veselinov K, Gioannini M, Piron R, Homeyer E, Even J, Loualiche S, and Montrosset I, *Proceedings of SPIE OPTO*, *Physics and Simulation of Optoelectronic Devices XVII, 72110Y, 7211,* **2009**, *San Jose, California, United States.*
12. Wang C, Gionnini M, Montrosset I, Even J, and Grillot F *Proceedings of SPIE OPTO, Physics and Simulation of Optoelectronic Devices XXIII, 93570L,* **2015***, San Francisco Jose, California, United States.*
13. Aleem M N A, Huessein K F A, and Ammar A A *Progress in Electromagnetics Research* **2013**, 28**,** 185.
14. Gioannini M, Rossetti M, *IEEE J. Sel. Topics Quantum Electron*. **2011**, 17**,** 1318.
15. Gioannini M, Bardella P, Montrosset I, *IEEE J. Sel. Topics Quantum Electron.* **2015,** 21**,** 1900811.
16. Veselinov K, Grillot F, Miska P, Homeyer E, Caroff P, Platz C, Even J, Dehaese O, Loualiche S, Marie X, and Ramdane A *Opt. Quantum Electron*. **2006**, 38, 369.
17. Xu D V, Yoon S F, and Tong C Z, *IEEE Journal of Quantum. Electronics.,* **2008**, 44**,** 879.
18. E. Avrutin,, B. Ryvkin, J. Kostamovaara, and D. Kuksenkov, *Semiconductor Science and Technology*, **2015**, 30**,** 055006.
19. Avrutin E. A, Dogru N, Ryvkin B, and Kostamovaara J T, *IET Optoelectronics,* **2016***,* 10**,** 57.
20. Dogru N, and Adams M J, *IEEE/OSA Journal of Lightwave Technology,* **2014**, 32, 3215.
21. Dogru N, and Adams M J , *IET Optoelectronics,* **2014**, 8, 44.
22. Veselinov K, Grillot F, Cornet C, Even J, Bekaiarski A, Gioannini M, and Loualiche S, *IEEE J. of Quantum Electron.* **2007**, 43**,** 810.
23. Bhattacharya P, Klotzkin D, Qasaimeh O, Zhou W, Krishna S, and Zhu D, *IEEE J. Sel. Top. Quantum Electron.* **2000**, 6, 426.
24. Cornet C, Labbe C, Folliot H, Bertru N, Dehaese O, Even J, Le Corre A, Paranthoen C, Platz C, and Loualiche S *Appl. Phys. Lett.* **2004**, 85**,** 5685.
25. Hantschmann C, Vasil'ev P P , Chen S, Liao M, Seeds A J, Liu H, Penty R V and White I H, *IEEE/OSA Journal of Lightwave Technology,* **2018**, 36, 3837.
26. Dogru N, Duranoglu Tunc H S, Al-Dabbagh A M, *Optics and Laser Technology* **2022**, 148, 107709.
27. Paranthoen C, Bertru N, Dehaese O, Loualiche S, and Lmabert B *Appl. Phys. Lett.* **2001**, 78**,** 1751.
28. Koenraad P M, Bertru N, Bimberg D, and Loualiche S, *Phys. Rev. B,* **2006***,* 74, 035312.

Author Contributions: Methodology, N.D.; software, H.T., E.C.; investigation, ND, H.T, E.C.; writing—original draft preparation, N.D.; supervision, N.D.; project administration, N.D. All authors have read and agreed to the published version of the manuscript.

Funding: This research was funded by The Scientific and Technological Research Council of Turkey (TUBITAK), grant number 119F099.

Data Availability Statement: Not applicable.

Conflicts of Interest: The authors declare no conflict of interest.